Inorg. Chem. **1987**, *26*, 203–205

Contribution from the Department of Chemistry and Center for Fundamental Materials Research,
Michigan State University, East Lansing, Michigan 48824

Anionic Photocatalysts Supported in Layered Double Hydroxides: Intercalation and Photophysical Properties of a Ruthenium Complex Anion in Synthetic Hydrotalcite

Emmanuel P. Giannelis, Daniel G. Nocera,* and Thomas J. Pinnavaia*

Received August 4, 1986

Immobilization of a photoactive complex anion within a layered system has been observed for the first time. Addition of aluminum and magnesium chloride salts ($AlCl_3$:$MgCl_2$ 2:1 w/w) to NaOH solutions containing the luminescent anion $Ru(BPS)_3^{4-}$ (BPS = 4,7-diphenyl-1,10-phenanthrolinedisulfonate) produces a hydrotalcite-like layered double hydroxide with a unit cell formula of $[Mg_{2.98}Al_{1.04}(OH)_8][Ru(BPS)_3]_{0.07}Cl_{0.72}\cdot yH_2O$. A basal spacing of 22 Å indicates the intercalated $Ru(BPS)_3^{4-}$ ions to be oriented with their C_3 axes normal to the double hydroxide layers. Electronic absorption, emission, and vibrational spectroscopies reveal that the structure of the $Ru(BPS)_3^{4-}$ ion is unperturbed by the interlayer environment. Emission decay profiles of the luminescent intercalate display multiexponential form due to excited-state self-quenching processes. Co-intercalation of $Ru(BPS)_3^{4-}$ with $Zn(BPS)_3^{4-}$ effectively increases the distance between $Ru(BPS)_3^{4-}$ ions within the hydrotalcite gallery, and accordingly, a diminution in the self-quenching reaction rate is observed with increasing $Zn(BPS)_3^{4-}$:$Ru(BPS)_3^{4-}$ ratios.

Recent photochemical studies of luminescent inorganic cations intercalated in smectite clays[1-5] suggest that this family of 2:1 phyllosilicates is a promising crystalline medium for mediating the reactivity of electronically excited metal complexes. Although a variety of smectite clays is available,[6,7] their versatility as solid-state photocatalysts is limited by their inability to intercalate anionic complexes. This is especially problematic in view of the potential photocatalytic importance of anionic polynuclear metal complexes, such as the heteropoly metalates[8-12] and complexes with metal–metal-bonded cores,[13-15] which derive their reactivity from metal centers in low formal oxidation states. The present work reports our initial efforts to form intercalation compounds wherein a luminescent complex anion is immobilized in the galleries of a layered inorganic host. Our approach utilizes the intercalation properties of a hydrotalcite-like layered double hydroxide and the photophysical properties of the complex anion $Ru(BPS)_3^{4-}$, where BPS is the sulfonated bathophenanthroline ligand 4,7-diphenyl-1,10-phenanthrolinedisulfonate.

In hydrotalcite and related layered double hydroxides (LDH's) the charge on the layers and gallery ions is the reverse of that for smectite clays. The positive charge on the layers results from the replacement of divalent cations by trivalent cations in brucite-like ($Mg(OH)_2$-type) octahedral sheets. Typical chemical compositions lie in the range $[M^{II}_{1-x}M^{III}_x(OH)_2]A_{x/n}^{n-}\cdot yH_2O$, where x = 0.20–0.33 and A^{n-} is the gallery anion.[16] In the mineral hydrotalcite,[17,18] $M^{II} = Mg^{2+}$, $M^{III} = Al^{3+}$, and $A^{n-} = CO_3^{2-}$. Synthetic hydrotalcite derivatives are prepared by precipitating the double hydroxide in the presence of anions including halide, nitrate, sulfate,[19,20] and simple tetrahedral and octahedral transition-metal anions[21,22] such as CrO_4^{2-} and $Fe(CN)_6^{4-}$.

Coprecipitation of Mg/Al LDH from an aqueous NaOH solution (pH ~10) containing the metal chloride salts and $Ru(BPS)_3^{4-}$ yields a red solid.[23,24] Subsequent hydrothermal treatment produces a microcrystalline product with a unit cell formula of $[Mg_{2.98}Al_{1.04}(OH)_8][Ru(BPS)_3]_{0.07}Cl_{0.72}\cdot yH_2O$ and a basal spacing of 22 Å. The observed spacing is in agreement with the value expected for a brucite-like layer (4.8 Å) plus a monolayer of $Ru(BPS)_3^{4-}$ with the C_3 axis of the complex normal to the hydroxide layers. In this orientation the ancillary sulfonate groups, which are situated at the vertices of a trigonal antiprism, are proximate to the hydrotalcite layers, thereby minimizing the charge separation between the positive layers and gallery anions. To our knowledge $Ru(BPS)_3^{4-}$ is the first photoactive anion to be intercalated in a layered host.

The visible absorption profile of $Ru(BPS)_3^{4-}$ is affected marginally upon incorporation in the galleries of hydrotalcite. As illustrated in Figure 1, the energy and absorption cross section for the metal-to-ligand charge-transfer transition centered at 450 nm are similar under intercalated conditions and in homogeneous solution. Conversely, the ligand-centered $\pi \rightarrow \pi^*$ absorption band at 285 nm exhibits a low-energy shoulder, and a significant decrease in absorption cross section upon intercalation. Similar perturbations for $Ru(bpy)_3^{2+}$ in smectite clays have been attributed, in part, to distortions of bipyridyl ligands.[2] However, for our LDH intercalate, the resonance Raman bands due to the

---

(1) (a) Krenske, D.; Abdo, S.; Van Damme, H.; Cruz, M.; Fripiat, J. J. *J. Phys. Chem.* **1980**, *84*, 2447–2457. (b) Nijs, H.; Fripiat, J. J.; Van Damme, H. *J. Phys. Chem.* **1983**, *87*, 1279–1282. (c) Nijs, H.; Cruz, M. I.; Fripiat, J. J.; Van Damme, H. *Nouv. J. Chim.* **1983**, *6*, 551–557.

(2) Della Guardia, R. A.; Thomas, J. K. *J. Phys. Chem.* **1983**, *87*, 990–998.

(3) Detellier, C.; Villemure, G. *Inorg. Chim. Acta* **1984**, *86*, L19–L20.

(4) Ghosh, P. K.; Bard, A. J. *J. Phys. Chem.* **1984**, *88*, 5519–5526.

(5) Suib, S. L.; Carrado, K. A. *Inorg. Chem.* **1985**, *24*, 863–867.

(6) Pinnavaia, T. J. *Science (Washington, D.C.)* **1983**, *220*, 365–371.

(7) Thomas, J. M. In *Intercalation Chemistry*; Whittingham, M. S., Jacobson, A. J., Eds.; Academic: New York, 1982; Chapter 3.

(8) Hill, C. L.; Bouchard, D. A. *J. Am. Chem. Soc.* **1985**, *107*, 5148–5157.

(9) Ioannidis, A.; Papaconstantinou, E. *Inorg. Chem.* **1985**, *24*, 439–441.

(10) Akid, R.; Darwent, J. R. *J. Chem. Soc., Dalton Trans.* **1985**, 395–399.

(11) Ward, M. D.; Brazdil, J. F.; Graselli, R. K. *J. Phys. Chem.* **1984**, *88*, 4210–4213.

(12) Yamase, T.; Takabayashi, N.; Kaji, M. *J. Chem. Soc., Dalton Trans.* **1984**, 793–799.

(13) (a) Nocera, D. G.; Maverick, A. W.; Winkler, J. R.; Che, C.-M.; Gray, H. B. *ACS Symp. Ser.* **1983**, *No. 211*, 21–33. (b) Maverick, A. W.; Najdzionek, J. S.; MacKenzie, D.; Nocera, D. G.; Gray, H. B. *J. Am. Chem. Soc.* **1983**, *105*, 1878–1882. (c) Nocera, D. G.; Gray, H. B. *Inorg. Chem.* **1984**, *23*, 3686–3688.

(14) Vogler, A.; Kunkely, H. *Inorg. Chem.* **1984**, *23*, 1360–1363.

(15) Roundhill, D. M. *J. Am. Chem. Soc.* **1985**, *107*, 4354–4356.

(16) Miyata, S. *Clays Clay Miner.* **1980**, *28*, 50–56.

(17) Allman, R.; Jepsen, H. P. *Neues Jahrb. Mineral, Monatsh.* **1969**, 544–551.

(18) Gastuche, M. C.; Brown, G.; Mortland, M. M. *Clay Miner.* **1967**, *7*, 177–192.

(19) Miyata, S. *Clays Clay Miner.* **1983**, *31*, 305–310.

(20) Miyata, S. *Clays Clay Miner.* **1975**, *23*, 369–375.

(21) Miyata, S.; Okada, A. *Clays Clay Miner.* **1977**, *25*, 14–18.

(22) Miyata, S.; Hirose, T. *Clays Clay Miner.* **1978**, *26*, 441–447.

(23) The $Ru(BPS)_3^{4-}$ intercalate was synthesized according to the following procedure. $K_4[Ru(BPS)_3]$[24] (0.50 g, 0.30 mmol), $MgCl_2\cdot 6H_2O$ (0.73 g, 3.6 mmol) and $AlCl_3\cdot 6H_2O$ (0.29 g, 1.2 mmol) were dissolved in 100 mL of degassed water. The pH was adjusted to 10.0 with 1.5 N NaOH, and the suspension was heated for 12 h under Ar at reflux temperature. The resulting intercalate was collected by centrifugation, washed, and air-dried.

(24) The potassium salt of $Ru(BPS)_3^{4-}$ was prepared by a modification of the method of Lin and co-workers (Lin, C.-T.; Bottcher, W.; Chou, M.; Creutz, C.; Sutin, N. *J. Am. Chem. Soc.* **1976**, *98*, 6536–6544). A 1-mL solution of BPS^{2-} ligand (0.50 g) was added with stirring to $RuCl_3\cdot 3H_2O$ (0.50 g) dissolved in 2 mL of H_2O. The mixture was heated to boiling for 25 min to produce a green solution. Reduction of the metal was accomplished with the addition of 0.5 mL of hypophosphorus acid followed by gently heating the solution for an additional 25 min. The solution volume was reduced to 3 mL, and a red-orange precipitate formed with the dropwise addition of a saturated KCl solution. The product was recrystallized from H_2O:MeOH solvent mixtures.

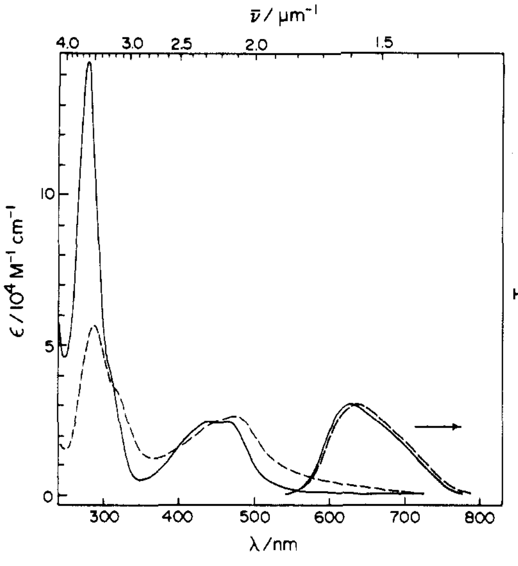

Figure 1. Absorption and emission spectra (λ_{exc} = 437 nm) of Ru(BPS)$_3^{4-}$ in H_2O (—) and Ru(BPS)$_3^{4-}$–hydrotalcite intercalate (- - -) at 25 °C. The spectra were recorded on H_2O suspensions of the hydrotalcite intercalate in which 30% of the exchange equivalents were replaced by Ru(BPS)$_3^{4-}$ ion.

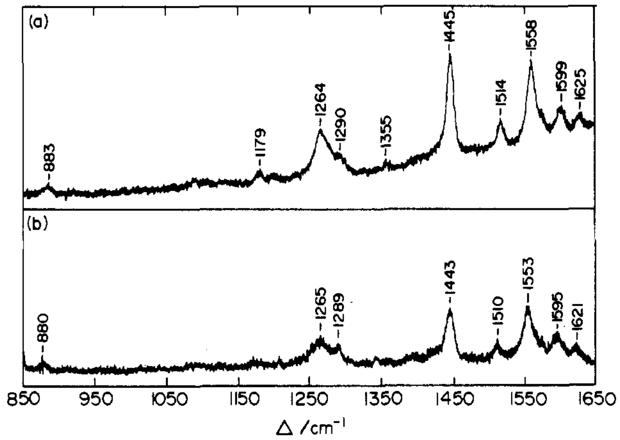

Figure 2. Resonance Raman spectra (λ_{exc} = 451.9 nm) of Ru(BPS)$_3^{4-}$ in (a) H_2O and (b) hydrotalcite (30% loading).

symmetric C–C and C–N stretching vibrations of the BPS ligand are little shifted relative to homogeneous solution (cf. Figure 2). A similar correlation is observed for the IR-active C–C, C–N, and S–O stretching vibrations. Thus, while low-symmetry-ligand distortions in the spatially restricted environment of LDH galleries could lead to a splitting of the $\pi \rightarrow \pi^*$ band, the congruence of the Raman and IR spectra for Ru(BPS)$_3^{4-}$ in solution and in the intercalated state, along with the relative insensitivity of the MLCT band to the interlayer environment, suggests such distortions to be small.

Consistent with visible absorption spectra, the steady-state luminescence of Ru(BPS)$_3^{4-}$ in hydrotalcite exhibits a profile that is slightly red-shifted relative to that for the complex in deaerated aqueous solution (cf. Figure 1). In contrast, time-resolved luminescence measurements reveal considerable differences between the emission lifetimes of Ru(BPS)$_3^{4-}$ in solution and in the intercalate. While irradiation (second harmonic Nd:YAG, fwhm = 8 ns) of aqueous solutions of Ru(BPS)$_3^{4-}$ yield luminescence decay curves obeying first-order kinetics ($\tau = 5.32 \times 10^{-6}$ s at 298 K), the luminescence decay of Ru(BPS)$_3^{4-}$ in the LDH is considerably more complex, exhibiting multiexponential form. In the long time limit the curve approaches exponential form with a lifetime of 2.60×10^{-6} s. At shorter times a faster and more complicated decay is observed, which can be fit to an additional exponential with a time constant of 0.32×10^{-6} s.[25] Analogous multiexponential luminescence decays of metal ions and complexes in smectites have been ascribed to quenching of the adsorbed excited state by impurity ions (e.g. Fe^{3+}, Cr^{3+}) isomorphically substituting for aluminum or silicon in the clay structure.[26] Similar impurity ion quenching for synthetic hydrotalcite is precluded by the exclusive presence of Mg^{2+} and Al^{3+} ions in the hydroxide layers.

Table I. Emission Lifetimes of Ru(BPS)$_3^{4-}$ Intercalate for Different Ru(BPS)$_3^{4-}$:Zn(BPS)$_3^{4-}$ Molar Ratios

Ru(BPS)$_3^{4-}$:Zn(BPS)$_3^{4-}$ [a]	$\tau/\mu s$ [b]
1:0	0.544 (0.54), 2.96 (0.46)[c]
1:1	4.31
1:9	5.60

[a] Hydrotalcite intercalates with 17% exchange capacity replaced by Ru- and Zn-BPS ions in the given molar ratios. [b] Lifetime measurements in deaerated H_2O suspensions of the intercalate. Lifetimes were recorded by using the second harmonic of a Nd:YAG laser (λ_{exc} = 532 nm). [c] Decay profile can be fit to biexponential kinetics. Numbers in parentheses represent fractional contribution of lifetime to decay curve.

The high local concentrations of Ru(bpy)$_3^{2+}$ in smectite interlayers are known to promote efficient excited-state self-quenching processes, which lead to multiphasic emission decay.[4] In view of the structural analogies between smectite and LDH intercalates, we have determined the emission kinetics for hydrotalcite intercalates in which 17% of the exchange equivalents were replaced by mixtures of Ru(BPS)$_3^{4-}$ and the nonemissive Zn(BPS)$_3^{4-}$. Table I lists the Ru(BPS)$_3^{4-}$ emission lifetimes for various Ru(BPS)$_3^{4-}$:Zn(BPS)$_3^{4-}$ molar ratios (Ru:Zn). For Ru:Zn = 1:0 the emission profile is similar to that of a fully saturated clay (30% loading of Ru(BPS)$_3^{4-}$). That a decrease in the loading of luminescent probe does not alter the emission kinetics suggests that a high concentration of Ru(BPS)$_3^{4-}$ is maintained by ion segregation within the hydrotalcite galleries. Also, the data in Table I clearly show that co-intercalation of Zn(BPS)$_3^{4-}$ results in longer emission time decays, which approach exponential behavior with increasing replacement of Ru(BPS)$_3^{4-}$. At a Ru:Zn ratio of 1:9 where the separation between Ru centers is largest, the emission kinetics of intercalated Ru(BPS)$_3^{4-}$ are similar to those for the solution complex. These results imply that multiphasic Ru(BPS)$_3^{4-}$ emission decay in hydrotalcite arises from self-quenching processes.[27]

On the basis of the hydrotalcite layer charge density and the molecular dimensions of Ru(BPS)$_3^{4-}$, we conclude that the extent of intercalation is limited by the size of the complex and not by the LDH anion-exchange capacity. For the fully saturated LDH, the anion layer is comprised of a 2-D network of Cl^- and Ru(BPS)$_3^{4-}$ with the latter at closest contact. When this result is coupled with the long-lived excited state of Ru(BPS)$_3^{4-}$, which is nearly ten times longer than that of Ru(bpy)$_3^{2+}$ in smectites containing low iron impurities,[2,4,26] the observation of Ru(BPS)$_3^{4-}$ self-quenching in hydrotalcite is not an unreasonable one. Despite self-quenching processes, it is important to note that we observe relatively long excited-state lifetimes of Ru(BPS)$_3^{4-}$ in hydrotalcite galleries. Also, we have recently found that anions at or near the edge sites of layered double hydroxides are accessible for reaction with substrates from solution.[28] The ability of these layered systems to incorporate anionic molecular species while preserving excited-state lifetimes and allowing for their chemical accessibility presage their utilization as the first viable layered host systems for the intracrystal immobilization of anionic photocatalysts. We

---

(25) Decay curves were fit to the equation $y = ae^{k_1t} + be^{k_2t}$ by using the modified simplex method. Convergence of the fit, monitored by the sum of the squares of the residuals, yielded values for variables a, b, k_1, and k_2.

(26) (a) Bergaya, F.; Van Damme, H. *J. Chem. Soc., Faraday Trans. 2* **1983**, *79*, 505–518. (b) Habti, A.; Keravis, D.; Levitz, P.; Van Damme, H. *J. Chem. Soc., Faraday Trans. 2* **1984**, *80*, 67–83.

(27) Multiphasic lifetime decays arising from factors such as impurity emission and site or local symmetry effects should not exhibit a dependence on the Zn(BPS)$_3^{4-}$ co-intercalate concentration.

(28) Martin, K. J.; Pinnavaia, T. J. *J. Am. Chem. Soc.* **1986**, *108*, 541–542.

are presently investigating the photochemistry of several polynuclear transition-metal anions intercalated within hydrotalcite layered supports.

Acknowledgment. The support of this work by the National Science Foundation through Grants CHE-8306583 (T.J.P.) and CHE-8451680 (D.G.N.), the Exxon Education Foundation (D.G.N.), and the Michigan State University Center for Fundamental Materials Research is gratefully acknowledged. D.G.N. also acknowledges the Presidential Young Investigator Program.

Notes

Contribution from the Department of Chemistry
and Molecular Structure Center, Indiana University,
Bloomington, Indiana 47405

Conversion of Carbon Dioxide to Carbonate Using a Rhodium μ-Hydroxy Species

Eric G. Lundquist, Kirsten Folting, John C. Huffman,
and Kenneth G. Caulton*

Received August 4, 1986

Chemical conversion of carbon dioxide is a resource utilization problem of worldwide interest.[1,2] Nucleophilic attack on CO_2 is a frequently successful strategy, being the basis for C–C bond formation by the enzyme Rubisco (addition of CO_2 to ribulose bisphosphate to give a six-carbon product).[3] When the nucleophile is OH^- (or H_2O), carbonic anhydrase catalyzes the conversion of CO_2 to the HCO_3^-/CO_3^{2-} equilibrium system. This latter enzyme is currently thought to involve bicarbonate production by addition of a Zn^{II}–OH unit to triatomic CO_2.[4]

Numerous studies of relevance to the carbonic anhydrase function have been reported.[1] These generally involve reaction of CO_2 with a hydroxy ligand bound to a *single*, coordinatively saturated (18-valence-electron) metal cation. Detailed kinetic studies are consistent with direct formation of a C–O bond without the intermediacy of prior coordination of CO_2 to the metal. The work reported here describes the result of reaction of a *bridging* hydroxyl group with CO_2.

Experimental Section

General Procedures and Materials. All manipulations were carried out by using standard Schlenk and glovebox procedures under prepurified nitrogen or vacuum. Solvents were dried and deoxygenated by Na/benzophenone (THF) or P_2O_5 (CH_2Cl_2 and CD_2Cl_2). ^1H spectra were recorded on a Nicolet 360-MHz spectrometer at 25 °C and referenced to Me_4Si. ^{13}C NMR spectra were recorded on a Varian XL 300 at 25 °C and referenced to solvent. Mass spectra were recorded on a Kratos MS-80. Bone Dry CO_2 (Matheson) was used as received.

$(COD)_2Rh_2(OH)_2$. $(COD)_2Rh_2(OH)_2$ was prepared according to the published synthesis,[5] modified by dissolving the final product in benzene and filtering to remove traces of KOH and KCl.

$(COD)_6Rh_6(CO_3)_3$. A degassed THF solution (20 mL) of $(COD)_2Rh_2(OH)_2$ (500 mg, 1.1 mmol) was exposed to CO_2 (3 mmol, 1 atm). After being stirred for 30 min, the clear yellow solution became cloudy and, upon standing for an additional 3 h, deposited a bright yellow powder. Decanting the THF solvent yielded 275 mg (52%) of pure, air-stable $(COD)_6Rh_6(CO_3)_3$. IR (Fluorolube mull): 1530, 1365 cm^{-1} (identified by comparison with the spectra of $(COD)_6Rh_6(^{13}CO_3)_3$ and $(COD)_2Rh_2Cl_2$). ^1H NMR (CD_2Cl_2, 360 MHz): 4.00 (s), 2.55 (m), 1.70 (m) ppm. The electron-impact mass spectrum of this material shows peaks above m/e 390, due to $(COD)Rh_2(CO_3)_nO^+$ (n = 1, 2) and $(COD)_2Rh_2O_m(CO_3)_{2-m}^+$ (m = 0–2).

Table I. Crystal Data for $[((COD)Rh)_2CO_3]_3$

empirical formula	$C_{51}H_{72}O_9Rh_6$
color	yellow
cryst dimens, mm	0.15 × 0.15 × 0.15
space group	$P\bar{1}$
cell dimens (at −156 °C; 36 reflecns)	
a, Å	13.238 (3)
b, Å	15.553 (4)
c, Å	12.894 (3)
α, deg	107.61 (1)
β, deg	91.39 (1)
γ, deg	100.40 (1)
molecules/cell	2
vol, Å^3	2479.77
calcd density, g/cm^3	1.937
wavelength, Å	0.71069
mol wt	1446.56
linear abs coeff, cm^{-1}	19.8
no. of unique intensities	6488
no. with $F > 0.0$	6021
no. with $F > 3.0\sigma(F)$	5465
final residuals	
$R(F)$	0.0361
$R_w(F)$	0.0388
goodness of fit for last cycle	0.90
max Δ/σ for last cycle	0.05

$(COD)_6Rh_6(^{13}CO_3)_3$. The ^{13}C-enriched compound was prepared (as above) on a vacuum line by using $^{13}CO_2$ prepared from 90% enriched $Ba^{13}CO_3$ and concentrated H_2SO_4. ^{13}C NMR (CD_2Cl_2, 74 MHz): 167.0 (s), 75.5 (br m), 31.0 (s) ppm. IR (Fluorolube mull): 1464, 1315 cm^{-1}.

Molecular Weight Determination. Molecular weights were determined by using the method of Signer[6] in CH_2Cl_2 at 25 °C. In a typical experiment, 10 mg of $(COD)_6Rh_6(CO_3)_3$ was dissolved in approximately 3.5 mL of CH_2Cl_2. Triphenylphosphine was used as the reference compound. Readings were taken daily until an equilibrium was achieved (about 12 days). The ^1H NMR spectrum of the molecular weight sample was recorded at the end of this time period; it revealed that no decomposition had occurred. Three measurements were taken, giving molecular weights of 433, 522, and 461.

Crystallography of $(COD)_6Rh_6(CO_3)_3$. A suitable, almost equidimensional crystal grown by slow evaporation from a THF solution was selected and transferred to the goniostat and cooled to −156 °C for characterization and data collection using graphite-monochromated radiation and a diffractometer of local construction. A systematic search of a limited hemisphere of reciprocal space yielded a set of reflections that exhibited no symmetry of systematic extinctions. The choice of the centrosymmetric triclinic space group, $P\bar{1}$, was confirmed by the successful solution and refinenent of the structure. Characteristics of the data collection[7] ($6° \leq 2\theta \leq 45°$), processing, and refinement are given in Table I.

The structure was solved by a combination of direct-methods and heavy-atom Fourier techniques. Six Rh atoms were located by means of MULTAN78, and the remainder of the atoms were located in successive difference maps. Hydrogen atoms were visible in a difference map. All hydrogen atoms were introduced in calculated positions with d(C–H) = 0.95 Å and individual isotropic thermal parameters equal to 1 greater than the isotropic parameter of the attached carbon atom. Due to program limitations and a lack of interest in the hydrogen positions, the

---

(1) Palmer, D. A.; van Eldik, R. *Chem. Rev.* **1983**, *83*, 651.

(2) Dinjus, E. *Z. Chem.* **1983**, *23*, 237.

(3) (a) Schneider, G.; Branden, C.-I.; Lorimer, G. H. *J. Mol. Biol.* **1984**, *175*, 99. (b) Edwards, G.; Walker, D. A. *C_3,C_4 Mechanisms, and Cellular and Environmental Regulation, of Photosynthesis*; University of California Press: Berkeley, CA, 1983.

(4) Slebocka-Tilk, H.; Cocho, J. L.; Frakman, Z.; Brown, R. S. *J. Am. Chem. Soc.* **1984**, *106*, 2421.

(5) Uson, R.; Oro, L. A.; Cabeza, J. A. *Inorg. Synth.* **1985**, *23*, 126–130.

(6) (a) Signer, R. *Justus Liebigs Ann. Chem.* **1930**, *478*, 246. (b) Childs, C. E. *Anal. Chem.* **1954**, *12*, 1963–1964.

(7) Huffman, J. C.; Lewis, L. N.; Caulton, K. G. *Inorg. Chem.* **1980**, *19*, 2755.

0020-1669/87/1326-0205$01.50/0